Nuclear Engineering and Design 268 (2014) 10–17

Contents lists available at ScienceDirect

Nuclear Engineering and Design

journal homepage: www.elsevier.com/locate/nucengdes

Lattice Boltzmann simulation of natural convection heat transfer in an open enclosure filled with Cu–water nanofluid in a presence of magnetic field

Ahmed Kadhim Hussein [a,*], Hamid Reza Ashorynejad [b], Mohsen Shikholeslami [b], S. Sivasankaran [c]

[a] Department of Mechanical Engineering, College of Engineering, Babylon University, Babylon City, Iraq
[b] Faculty of Mechanical Engineering, Babol University of Technology, Babol, Mazandaran, Islamic Republic of Iran
[c] Institute of Mathematical Sciences, University of Malaya, Kuala Lumpur 50603, Malaysia

HIGHLIGHTS

- Convection very strong when *Ra* is high and *Ha* = 0.
- Isotherms smooth when *Ra* is low and *Ha* is high.
- Maximum stream function increases by adding nano-particle.
- Flow circulation decreases when magnetic orientation angle increases.
- Nusselt number ratio increases when *Ra* increases.

ARTICLE INFO

Article history:
Received 26 March 2013
Received in revised form 13 October 2013
Accepted 2 November 2013

ABSTRACT

In this paper magneto hydrodynamic (MHD) natural convection flow of Cu–water nanofluid in an open enclosure is investigated numerically using lattice Boltzmann method (LBM) scheme. The effective thermal conductivity and viscosity of nanofluid are calculated by the Maxwell–Garnetts (MG) and Brinkman models, respectively. In addition, the MDF model was used for simulating the effect of uniform magnetic field. The influence of pertinent parameters such as Hartmann number, nanoparticle volume fraction, Rayleigh number and the inclination of magnetic field on the flow and heat transfer characteristics have been examined. The results indicate that the absolute values of stream function decline significantly by increasing Hartmann numbers while these values rise by increasing Rayleigh numbers. Moreover, the results show that the solid volume fraction has a significant influence on stream function and heat transfer, depending on the value of Hartmann and Rayleigh numbers.

1. Introduction

Natural convection in enclosures occurs in numerous applications and has been studied extensively in the literature. In contrast, there is rather little work with open cavities, which constitute another important application area. Natural convection in open cavities is relevant in several thermal engineering applications. Some examples include the cooling of electronic devices and the design of solar concentrators receivers, among others. Chan and Tien (1985) studied numerically shallow fully open cavities and also made a comparison study using a square cavity in an enlarged computational domain. They found that for a square open cavity having an isothermal vertical side facing the opening and two adjoining adiabatic horizontal sides, satisfactory heat transfer results could be obtained, especially at high Rayleigh numbers. Polat and Bilgen (2002) investigated laminar natural convection in inclined open shallow cavities at different inclination angles. They found that the inclination angle of the heated plate was an important parameter which affecting volumetric flow rate and the heat transfer. Polat and Bilgen (2002) studied numerically inclined fully open shallow cavities in which the side facing the opening was heated by constant heat flux, two adjoining walls were insulated and the opening was in contact with a reservoir at constant temperature and pressure. The computational domain was restricted to the cavity. From the other side, natural convection under the influence of a magnetic field is of great importance in many industrial applications such as crystal growth, metal casting and liquid

* Corresponding author. Tel.: +964 7813769317.
E-mail addresses: ahmedkadhim7474@gmail.com, ahmedkadhim74@yahoo.com (A.K. Hussein).

0029-5493/$ – see front matter © 2014 Published by Elsevier B.V.
http://dx.doi.org/10.1016/j.nucengdes.2013.11.072

Nomenclature

B	magnetic flux density (T)
C_s	speed of sound in Lattice scale
e_α	discrete lattice velocity in direction i
F_{ext}	external force
f_k^{eq}	equilibrium distribution of flow field
g	internal energy distribution functions
g_{eq}	equilibrium internal energy distribution functions
g_y	acceleration due to gravity (m/s^2)
Gr	Grashof number ($= g\beta\Delta TH^3/\upsilon^2$)
Ha	Hartmann number ($= B_0(H)/\sqrt{\upsilon\eta}$)
k	thermal conductivity (W/m K)
L	height/width of the enclosure (m)
Nu	average Nusselt number
Nu^*	average Nusselt number ratio
Pr	Prandtl number ($=\upsilon/\alpha$)
Ra	Rayleigh number ($= g\beta\Delta T(H)^3/\alpha\nu$)
T	fluid temperature (K)
u, v	velocity components in the x-direction and y-direction respectively (m/s)

Greek symbols

η	magnetic resistivity
α	thermal diffusivity (m^2/s)
ϕ	solid volume fraction
μ	dynamic viscosity (kg/m s)
υ	kinematic viscosity (m^2/s)
τ	lattice relaxation time
θ	dimensionless temperature
ρ	fluid density (kg/m^3)
Ψ	dimensionless stream function
β	thermal expansion coefficient (K^{-1})
γ	magnetic field orientation angle ($^\circ$)
Δt	lattice time step
c	cold
h	hot
ave	hot
nf	nanofluid
n	base fluid

metal cooling blankets for fusion reactors. Ozoe and Okada (1989) reported a three-dimensional numerical study to investigate the effect of the magnetic field path in a cubical enclosure. Rudraiah et al. (1995) investigated numerically the effect of magnetic field on natural convection in a rectangular enclosure. They found that the magnetic field decreased the rate of heat transfer. Qi et al. (1999) studied natural convection in a cavity with partially heated from below in the presence of an imposed non-uniform magnetic field. They found that the velocity decreased with increasing the magnetic field strength. Mahmoudi et al. (2011) investigated numerical modeling of natural convection in an open enclosure with two vertical thin heat sources subjected to a nanofluid. They demonstrated that the average Nusselt number increased linearly with the increase in the solid volume fraction of nanoparticles. Most of the studies on the natural convection in enclosures with the magnetic effects have considered the electrically conducting fluid with a low thermal conductivity. This, in turn, limits the enhancement of heat transfer in the enclosure particularly in the presence of the magnetic field. Nanofluids with enhanced thermal characteristics have widely been examined to improve the heat transfer performance of many engineering applications. Due to the increasing importance of nanofluids, in recent years, some interest has been given to the study of convective transport of nanofluids. The convection heat transfer rate in fluids such as oil, water and ethylene glycol mixture is poor, since the thermal conductivity of these fluids plays an important role on the heat transfer coefficient between the heat transfer medium and the heat transfer surface. Therefore numerous methods were proposed to improve the thermal conductivity of these fluids by suspending nano/micro (larger-size) particle materials in liquids (Kakaç and Pramuanjaroenkij, 2009). Khanafer et al. (2003) firstly conducted a numerical investigation on the heat transfer enhancement due to adding nano-particles in a differentially heated enclosure. They found that the suspended nanoparticles substantially increased the heat transfer rate at any given Grashof number. As discussed earlier, the magnetic field leads to the reduction of convective circulating flows within the enclosures filled with electrically conducting fluids. This, in turn, decreases the heat transfer rate. The addition of nanoparticles to the fluid can improve its thermal performance and enhance the heat transfer mechanism in the enclosure. In some engineering problems such as the magnetic field sensors, the magnetic storage media and the cooling systems of electronic devices, enhanced heat transfer was desirable whereas the magnetic field weakened the convection flow field. In order to improve the heat transfer performance of such devices, the use of nanofluids with higher thermal conductivity can be considered as a promising solution. One of the useful numerical methods that have been used in the recent years is the lattice Boltzmann method. It was used for simulation the flow field in wide ranges of the engineering applications such as natural convection, porous media, nanofluid flow, and MHD flow. Bararnia et al. (2011) numerically investigated natural convection in a nanofluids-filled portioned cavity using lattice-Boltzmann method. They found that the partition inclination increased the heat transfer rate so that the vertical partition offered the highest heat transfer rate. Several works have been studied by this method in simulating natural convection recently (Nemati et al., 2011; Aghajani Delavar et al., 2011). There are two lattice Boltzmann models for MHD flows: the multi-speed (MS) model and multi-distribution-function (MDF) model. In MS model, the equilibrium distribution was transformed in order not only to include the magnetic field force, but also to be equal to the magnetic field vector on a different vector base. This was achieved by allowing an extra degree of freedom and by defining supplementary vectors on each base vector. Combining the base and the supplementary vectors, the two vector bases are defined for the momentum and the magnetic field (Chang Feng et al., 2005; MacNab et al., 2001). In the MDF model presented by Dellar (2002), the Lorentz force can be introduced as a pointwise force, the induction equation was also solved using an LBGK equation by introducing an independent distribution function. MDF models can improve the numerical stability. The accuracy of the MDF models has been verified by several benchmark studies (Xing-Wang and Bao Chang, 2005; Hasanpour et al., 2010). This paper presents application of lattice Boltzmann method for MHD flow of Cu–water nanofluid in an open enclosure. The effective thermal conductivity and viscosity of nanofluid are calculated using the Maxwell–Garnetts (MG) and Brinkman models, respectively. In addition, the MDF model is used for simulating the effect of uniform magnetic field. The effects of Hartmann number, nanoparticle volume fraction, Rayleigh number and the magnetic field inclination on the flow and heat transfer characteristics have been examined.

2. Problem definition and mathematical model

2.1. Problem statement

The geometry of the present problem is shown in Fig. 1. It displays a two-dimensional enclosure with height and width of (H).

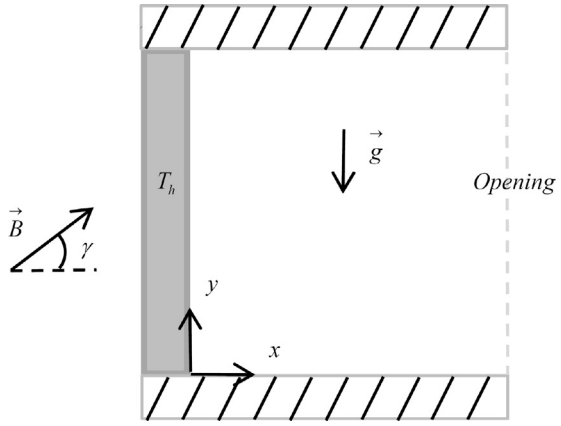

Fig. 1. Geometry of the problem.

The temperature of the enclosure left sidewall is maintained at (T_h). An external cold nanofluid enters into the enclosure from the right (east) opening boundaries while the copper–water nanofluid is correlated with the opening boundary at constant temperature (T_c). The top and bottom horizontal walls have been considered to be adiabatic, i.e., non-conducting and impermeable to mass transfer. The enclosure is filled with a Cu–water nanofluid and is influenced by a uniform magnetic field (B) at different orientation angles ($\gamma = 0^\circ, 30^\circ, 60^\circ$ and 90°). The Hartmann number is varied as ($Ha = 0$, 20, 40 and 60) while the Rayleigh number is varied as ($Ra = 10^4$, 10^5 and 10^6). The flow is considered to be steady, two dimensional and laminar, and the radiation effects are negligible. The displacement currents, induced magnetic field, dissipation and Joule heating are also neglected.

2.1.1. The lattice Boltzmann method

The LB model used here is the same as that employed in Mohamad et al. (2009). The thermal LB model utilizes two distribution functions, f, g and B, for the flow, temperature and magnetic fields, respectively. It uses modeling of movement of fluid particles to capture macroscopic fluid quantities such as velocity, pressure, temperature and magnetic field. In this approach, the fluid domain was discretized to uniform Cartesian cells. Each cell holds a fixed number of distribution functions, which represents the number of fluid particles moving in these discrete directions. The D2Q9 model was used and values of $w_0 = 4/9$ for $|c_0| = 0$ (for the static particle), $w_{1-4} = 1/9$ for $|c_{1-4}| = 1$ and $w_{5-9} = 1/36$ for $|c_{5-9}| = \sqrt{2}$ are assigned in this model.

The density and distribution functions, i.e., the f, g and B are calculated by solving the lattice Boltzmann equation (LBE), which is a special discretization of the kinetic Boltzmann equation. After introducing BGK approximation, the general form of lattice Boltzmann equation with external force is: for the flow field:

$$f_i(x + c_i\Delta t, t + \Delta t) = f_i(x, t) + \frac{\Delta t}{\tau_v}\left[f_i^{eq}(x, t) - f_i(x, t)\right] + \Delta t c_i F_k \quad (1)$$

For the temperature field:

$$g_i(x + c_i\Delta t, t + \Delta t) = g_i(x, t) + \frac{\Delta t}{\tau_C}\left[g_i^{eq}(x, t) - g_i(x, t)\right] \quad (2)$$

where Δt denotes lattice time step, c_i is the discrete lattice velocity in direction i, F_k, is the external force in direction of lattice velocity, τ_v and τ_C denotes the lattice relaxation time for the flow and temperature fields. The kinetic viscosity c and the thermal diffusivity α, are defined in terms of their respective relaxation times, i.e., $\upsilon = c_s^2(\tau_v - 1/2)$ and $\alpha = c_s^2(\tau_C - 1/2)$, respectively. Note that the limitation $0.5 < \tau$ should be satisfied for both relaxation times to ensure that viscosity and thermal diffusivity are positive. Furthermore, the local equilibrium distribution function determines the type of problem that needs to solve. It also models the equilibrium distribution functions for flow and temperature fields respectively. In this study, the density distribution function, f_i^{eq}, is modified to consider the magnetic effect:(3)$f_i^{eq} = w_i\rho\left[1 + \frac{c_i\cdot u}{c_s^2} + \frac{1}{2}\frac{(c_i\cdot u)^2}{c_s^4} - \frac{1}{2}\frac{u^2}{c_s^2}\right] + \frac{w_i}{2c_s^2}\left[\frac{B^2c^2}{2} - (c\cdot B)^2\right]$

$$g_i^{eq} = w_i T\left[1 + \frac{c_i\cdot u}{c_s^2}\right] \quad (4)$$

where B is the magnetic field, w_i is weighting factor, c_s is the speed of sound and defined by $c_s = c/\sqrt{3}$. Similarly, to density equilibrium function (f_i^{eq}), for calculating the magnetic field, magnetic equilibrium function considered as following (MacNab et al., 2001):

$$h_{ix}^{eq} = \lambda_i\left[B_x + \frac{1}{c_s^2}e_{ix}(u_yB_x - u_xB_y)\right] \quad (5)$$

$$h_{iy}^{eq} = \lambda_i\left[B_y + \frac{1}{c_s^2}e_{iy}(u_xB_y - u_yB_x)\right] \quad (6)$$

where λ_i is the weighting factor of magnetic field and defined in fifth direction by (MacNab et al., 2001):

$$\lambda_i = \begin{cases} \frac{1}{3} & \text{for } i = 0 \\ \frac{1}{6} & \text{for } i = 1-4 \end{cases} \quad (7)$$

For solving the velocity and magnetic field, the following equation must be considered (MacNab et al., 2001):

$$h_i(x + c_i\Delta t, t + \Delta t) = h_i(x, t) + \frac{\Delta t}{\tau_m}\left[h_i^{eq}(x, t) - h_i(x, t)\right] \quad (8)$$

The magnetic resistivity, like kinetic viscosity υ and the thermal diffusivity α, defined in terms of its respective relaxation time $\eta = c_s^2(\tau_m - 1/2)$.

In order to incorporate buoyancy force in the model, the force term in the Eq. (1) needs to calculate as below in the vertical direction (y):

$$F = 3w_ig_y\beta\theta \quad (9)$$

For natural convection, the Boussinesq approximation is applied and radiation heat transfer is negligible. To ensure that the code works in near incompressible regime, the characteristic velocity of the flow for natural ($V_{\text{natural}} \equiv \sqrt{\beta g_y \Delta T H}$) regime must be small compared with the fluid speed of sound. In the present study, the characteristic velocity selected as 0.1 of sound speed.

Finally, macroscopic variables are calculated using the following formula:

$$\rho = \sum_i f_i, \quad \rho u = \sum_i c_i f_i, \quad T = \sum_i g_i, \quad B_x = \sum_i h_{ix}, \quad B_y = \sum_i h_{iy} \quad (10)$$

2.2. Boundary conditions

2.2.1. Flow field

Implementation of boundary conditions is very important for the simulation. The unknown distribution functions pointing to the fluid zone at the boundaries nodes must be specified. Concerning the no-slip boundary condition, bounce back boundary condition

Table 1
Thermo physical properties of water and nanoparticles (Xuan and Roetzel, 2000).

Properties	ρ (kg/m^3)	C_p (j/kg k)	k (W/m k)	$\beta \times 10^5$ (K^{-1})
Pure water	997.1	4179	0.613	21
Copper (Cu)	8933	385	401	1.67

is used on the solid boundaries. The unknown density distribution functions at the east (right) boundary (open boundary) can be determined by the following conditions:

$$f_{6,n} = f_{6,n-1}, \quad f_{7,n} = f_{7,n-1}, \quad f_{3,n} = f_{3,n-1} \tag{11}$$

2.2.2. Temperature field

The top and bottom enclosure boundaries are adiabatic so bounce back boundary condition is used on them. Temperatures at the left and right walls are known. In the left (west) wall $T_h = 1$. Since we are using D2Q9, the unknown internal energy distribution function at the left and right boundaries can be determined by the following conditions (Mohamad et al., 2009):

For the left (west) wall

$$g_{1,0} = T_h(w(1) + w(3)) - g_{3,0} \tag{12}$$

For the right (east) wall

$$\begin{aligned} &\text{if } u < 0 \quad \text{then}: \quad g_{3,n} = -g_{1,n}, \quad g_{6,n} = -g_{8,n}, \quad g_{7,n} = -g_{5,n} \\ &\text{if } u > 0 \quad \text{then}: \quad g_{3,n} = g_{3,n-1}, \quad g_{6,n} = g_{6,n-1}, \quad g_{7,n} = g_{7,n-1} \end{aligned} \tag{13}$$

2.3. The Lattice Boltzmann model for nanofluid

In order to simulate the nanofluid by the lattice Boltzmann method, because of the interparticle potentials and other forces on the nanoparticles, the nanofluid behaves differently from the pure liquid from the mesoscopic point of view and is of higher efficiency in energy transport as well as better stabilization than the common solid–liquid mixture. For pure fluid in absence of nanoparticles in the enclosures, the governing equations are Eqs. ((1)–(13)). However for modeling the nanofluid because of changing in the fluid thermal conductivity, density, heat capacitance and thermal expansion, some of the governing equations should change. The nanofluid is a two component mixture modeled as a single-phase incompressible fluid. Physical properties given by Table 1 (Oztop and Abu-Nada, 2008).

The effective density $\rho_{n,f}$, the effective heat capacity $(\rho C_p)_{nf}$ and thermal expansion$(\rho\beta_p)$of the nanofluid are defined as (Xuan and Roetzel, 2000):

$$\rho_{nf} = \rho_f(1-\phi) + \rho_s\phi \tag{14}$$

$$(\rho C_p)_{nf} = (\rho C_p)_f(1-\phi) + (\rho C_p)_s\phi \tag{15}$$

$$(\rho\beta)_{nf} = (\rho\beta)_f(1-\phi) + (\rho\beta)_s\phi \tag{16}$$

where (ϕ) is the solid volume fraction of the nanoparticles and subscripts *f*, *nf* and *s* refer for base fluid, nanofluid and solid, respectively.

The viscosity of the nanofluid containing a dilute suspension of small rigid spherical particles is (Brinkman model, Wang and Mujumdar, 2007):

$$\mu_{nf} = \frac{\mu_f}{(1-\phi)^{2.5}} \tag{17}$$

The effective thermal conductivity of the nanofluid can be approximated by the Maxwell–Garnetts (MG) model as (Abu-Nada et al., 2008):

$$\frac{k_{nf}}{k_f} = \frac{k_s + 2k_f - 2\phi(k_f - k_s)}{k_s + 2k_f + \phi(k_f - k_s)} \tag{18}$$

Table 2
Comparison of average Nusselt number at the hot left sidewall for different Rayleigh numbers when Pr = 0.7.

Ra	Present	FVM (Mohamad, 1995)
10^3	3.336	3.264
10^4	7.354	7.261
10^5	14.330	14.076

Average Nusselt number (Nu_{ave}) is one of the most important dimensionless parameters in the description of the convective heat transport. The local Nusselt number and the average value at the hot wall are calculated as:

$$Nu_{ave} = -\frac{k_{nf}}{k_f}\frac{1}{H}\int_0^H \left(\frac{\partial T}{\partial x}\right) dy \tag{19}$$

Because of the convenience, a normalized average Nusselt number is defined as the ratio of Nusselt number at any volume fraction of nanoparticles to that of pure water as follows:

$$Nu^*_{ave} = \frac{Nu_{ave}\big|_{\phi=0.06}}{Nu_{ave}\big|_{\phi=0}} \tag{20}$$

3. Code validation

In order to verify the accuracy of the present numerical study, the present numerical model was validated against the results obtained by Mohamad (1995) as shown in Table 2. In addition, Fig. 2 illustrates an excellent agreement between the present calculations and the results of Khanafer et al. (2003) for natural convection in an enclosure filled with Cu–water nanofluid. Furthermore, Fig. 3 shows the effect of a transverse magnetic field on natural-convection flow inside a rectangular enclosure which are compared with the result of Rudraiah et al. (1995). All of these favorable comparisons lend confidence in the accuracy of the present LBM code.

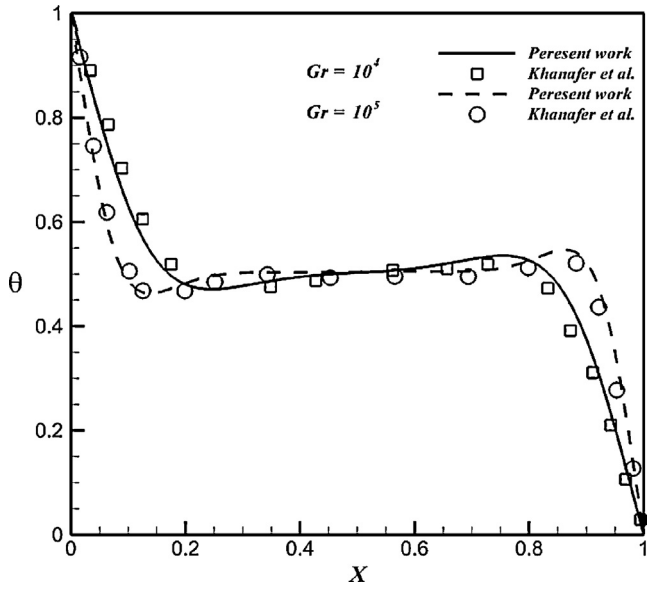

Fig. 2. Comparison of the temperature distribution on axial midline between the present results and numerical results by Khanafer et al. (2003) for $\phi = 0.1$ and $Pr = 6.8$ (Cu–water).

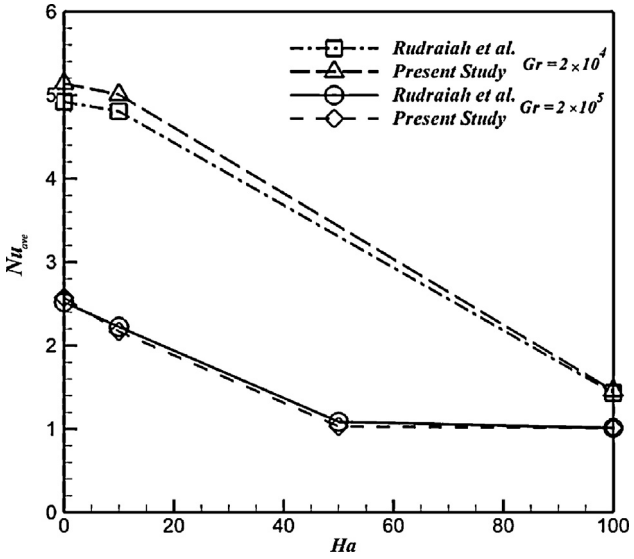

Fig. 3. Comparison of the average Nusselt number versus Hartmann number at different values of Grashof number.

4. Results and discussion

Fig. 4 shows streamlines (left) and isotherms (right) contours of the open enclosure for Cu–water nanofluid ($\varphi = 0.06$) and pure fluid ($\varphi = 0$) when $Ra = 10^6$, $L/t = 10$ and $Ha = 0$ (no magnetic field effect). It can be observed that, the external cold nanofluid enters into the enclosure from the right opening boundaries, flows along the bottom wall and then heated due to the buoyancy force along the hot left sidewall and finally leaves along the top wall. It is clear from this figure, that the streamlines and isotherms are distributed strongly in the enclosure due to the significant effect of the convection encountered when the Rayleigh number is high (i.e., $Ra = 10^6$). The another reason of high flow circulation intensity because the effect of magnetic field is negligible (i.e., $Ha = 0$). Moreover, due to the high Rayleigh number the center of re-circulating vortices shifts toward the hot left sidewall. For the same reason, it can be seen also that the isotherms contours accumulate strongly adjacent the hot left sidewall indicating that the heat is transferred by convection. Also, it can be noticed that the maximum stream function of nanofluid ($|\psi_{max}| = 0.407$) is greater than the corresponding value of pure fluid ($|\psi_{max}| = 0.289$). The reason of this phenomena because as the solid volume fraction increases, the nanoparticles velocity increases which leads to increase flow circulation and the thermal energy transport through the fluid.

Figs. 5–7 illustrate streamlines (left) and isotherms (right) contours for different values of Hartmann number ($Ha = 0$, 20, 40 and 60), $\varphi = 0.06$ (nanofluid), $\gamma = 0^\circ$ and ($Ra = 10^4$, 10^5 and 10^6) respectively. The Hartmann number represents a measure of the relative importance of MHD flow. It is clear from these figures, that the flow field of the nanofluid in the core of the enclosure is strongly influenced by increasing the magnetic field strength (i.e., increasing the Hartmann number). The maximum stream function of the nanofluid begins to decrease as the Hartmann number increases for all values of the Rayleigh number. This is because when the Hartmann number increases (i.e., $Ha = 20$, 40 and 60), the Lorentz force which is created due to the magnetic field effect becomes higher than the buoyancy force which causes to reduce the flow circulation intensity and as a result the convection effect begins to diminish. The higher value of the maximum stream function can be seen when the effect of magnetic field is negligible (i.e., $Ha = 0$). In this case, the strength of circulation is very strong, since the buoyancy

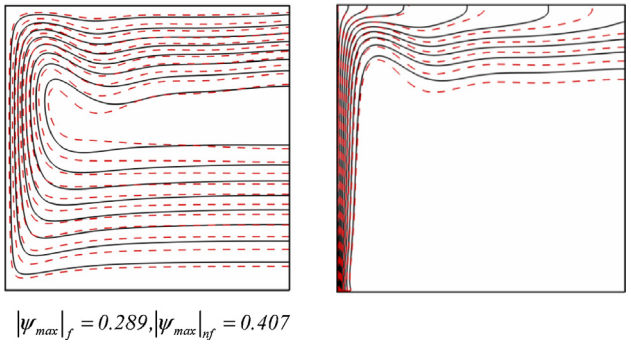

Fig. 4. Streamlines (left) and isotherms (right) contours between Cu–water nanofluid ($\phi = 0.06$) (- - -) and pure fluid ($\phi = 0$) (—) when $Ra = 10^6$, $Ha = 0$.

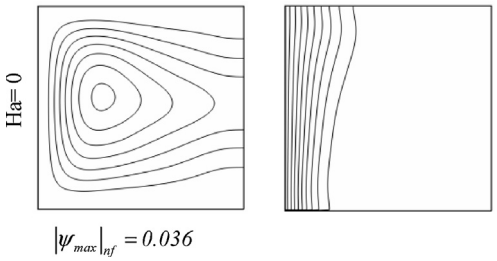

Fig. 5. Streamlines (left) and isotherms (right) contours for different values of Hartmann number (Ha) and at $Ra = 10^4$, $\phi = 0.06$ and $\gamma = 0^\circ$.

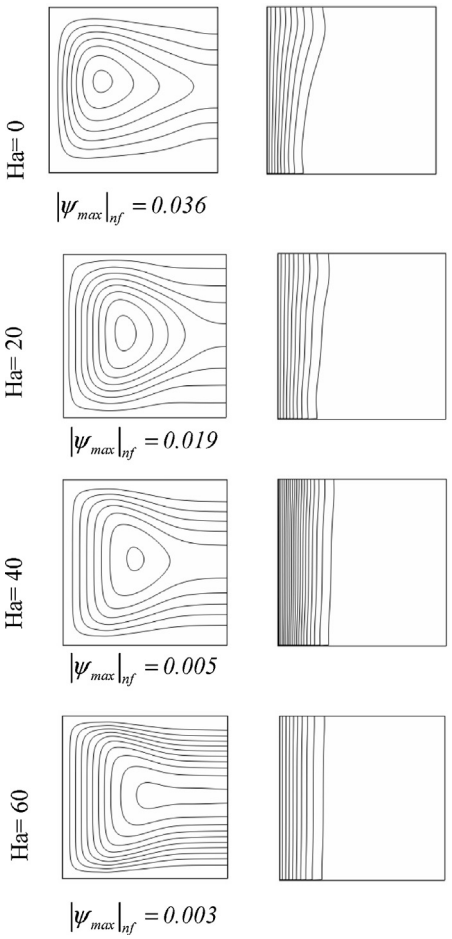

Fig. 6. Streamlines (left) and isotherms (right) contours for different values of Hartmann number (Ha) and at $Ra = 10^5$, $\phi = 0.06$ and $\gamma = 0^\circ$.

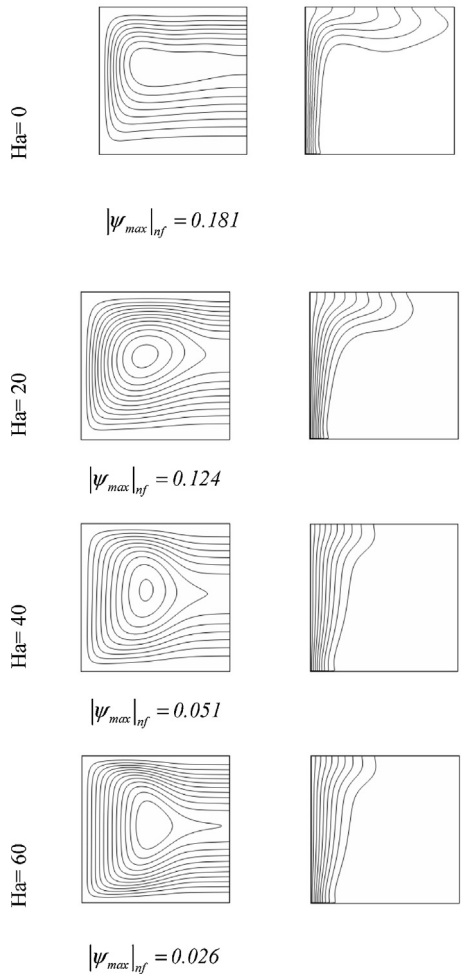

Fig. 7. Streamlines (left) and isotherms (right) contours for different values of Hartmann number (Ha) and at $Ra = 10^6$, $\phi = 0.06$ and $\gamma = 0^\circ$.

force due to natural convection effect is the only dominant force in the enclosure with the absence of magnetic field effect. From the other hand, it can be seen that the maximum stream function values increase as the Rayleigh number increases. Also, a clear confusion occurs in the shape of re-circulating vortices as the Rayleigh number increases, since the buoyancy forces are dominating over the viscous forces. This increasing in the Rayleigh number causes a significant jump in the flow circulation and leads to increase the maximum stream function values. In general, the flow field inside the enclosure can be represented by various re-circulating vortices which cover all the enclosure zone. The core of these vortices shifts toward the opening of the enclosure as the Rayleigh number increases. With respect to isotherms, when the Rayleigh number is low (i.e., $Ra = 10^4$ (Fig. 5)) or the Hartmann number is high (i.e., $Ha = 20$, 40 and 60), the isotherms are approximately linear and they are symmetrical and parallel to the hot left sidewall indicating that the heat is transferred by the conduction. The linearity of the isotherms begins very clear as the Hartmann number increases. This is because the magnetic field role is strong enough to reduce the convection effect inside the enclosure. No clear thermal boundary layer can be seen when the Rayleigh number is low. As the Rayleigh number increases (i.e., $Ra = 10^5$ and 10^6 (Figs. 6 and 7)) or when the magnetic field is negligible (i.e., $Ha = 0$), the isotherms are begin to confuse in shape, highly compressed and accumulate adjacent to the enclosure hot left sidewall indicating that the convection is the dominant mechanism for the heat transfer in the enclosure. These isotherms refer that a high temperature gradient

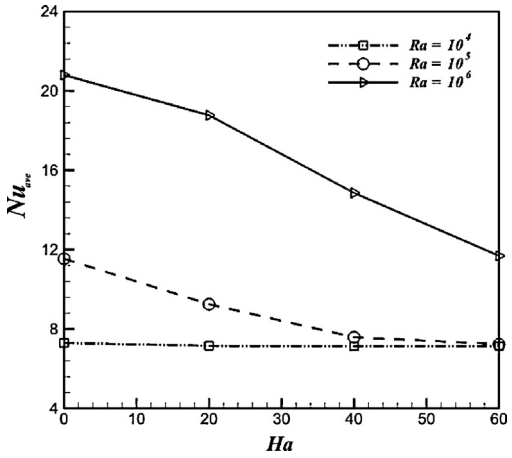

Fig. 8. Variation of average Nusselt number at different Hartmann number and Rayleigh number when $\phi = 0.06$ and $\gamma = 0^\circ$.

can be noticed between the cold nanofluid and the hot wall. In this case a thermal boundary layer can be found adjacent to the hot left side wall of the enclosure.

Fig. 8 demonstrates the variation of average Nusselt number at different Hartmann number and Rayleigh number when $\varphi = 0.06$ (nanofluid) and $\gamma = 0^\circ$. From this figure, it is noticed that the average Nusselt number increases dramatically when the Rayleigh number increases, especially when the Hartmann number is zero ($Ha = 0$). This is due to the increase in the intensity of the convection currents which causes a clear enhancement in the heat transfer rate represented by the average Nusselt number. When the Rayleigh number is low ($Ra = 10^4$), the average Nusselt number is almost has a constant behavior with the increase of the Hartmann number. This is because the buoyancy force effect is weak, so the convection heat transfer contribution is weak too and the conduction heat transfer is dominated. It is also found that the average Nusselt number is decreased as the Hartmann number increases. This is due to the reduction in the flow circulation and the temperature gradient when the Hartmann number increases. Therefore, the magnetic force is the dominant force and controls the flow inside the open enclosure causing to reduce the average Nusselt number.

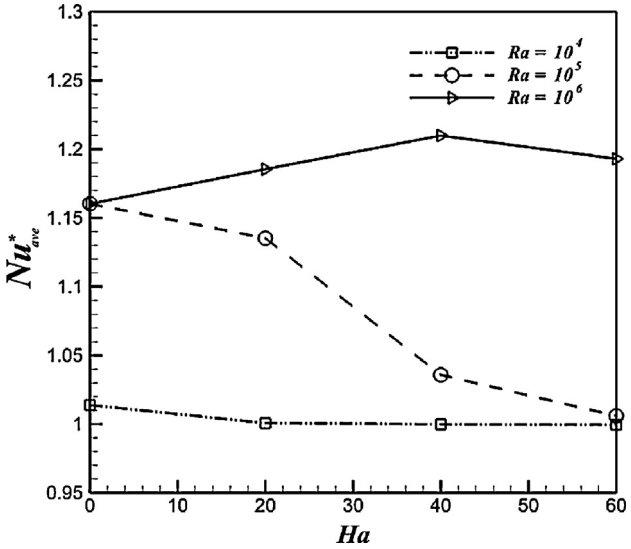

Fig. 9. Effects of Hartmann number and Rayleigh number on Nusselt number ratio ($(Nu^*_{ave} = Nu_{ave}|_{\phi=0.06} / Nu_{ave}|_{\phi=0})$) when $\phi = 0.06$ and $\gamma = 0^\circ$.

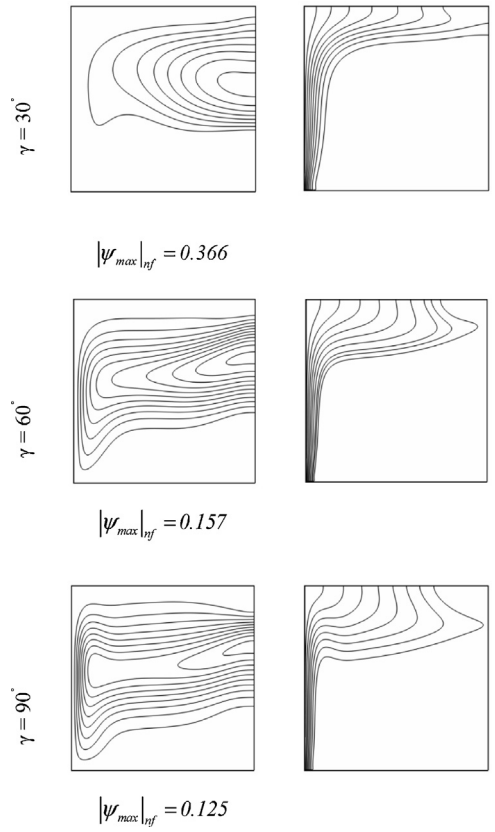

Fig. 10. Streamlines (left) and isotherms (right) contours for different values of (γ) and at $Ra = 10^6$, $\phi = 0.06$ and $Ha = 60$.

Fig. 9 presents the effects of Hartmann number and Rayleigh number on Nusselt number ratio (Nu^*_{ave}) when $\varphi = 0.06$ (nanofluid) and $\gamma = 0^\circ$. It can be noticed that, when the Rayleigh number increases, the Nusselt number ratio increases. This is because the buoyancy forces effect increases when the Rayleigh number increases. When ($Ra = 10^4$), an approximately constant variation can be seen of the Nusselt number ratio when the Hartmann number increases. For ($Ra = 10^5$), the Nusselt number ratio begins to decrease gradually as the Hartmann number increases. This is because the effect of magnetic field becomes significant when the Hartmann number increases. But, when ($Ra = 10^6$) a reverse behavior can be seen for the Nusselt number ratio when the Hartmann number increases up to ($Ha = 40$). This is due to the strong circulation encountered when ($Ra = 10^6$). Greater than ($Ha = 40$), the Nusselt number ratio begins to decrease again since for high Hartmann number, the magnetic force effect becomes greater than the buoyancy force effect and leads to reduce the Nusselt number ratio.

Fig. 10 displays contours of streamlines (left) and isotherms (right) for various values of magnetic field orientation angle ($\gamma = 30^\circ, 60^\circ$ and 90°) respectively, $Ra = 10^6$, $\varphi = 0.06$ (nanofluid) and $Ha = 60$. It can be observed that, when the magnetic field orientation angle increases from ($\gamma = 30^\circ$) to ($\gamma = 90^\circ$), the intensity of flow circulation and the convection role begin to decrease. This observation is very evident through the nanofluid maximum stream function values which begin to decrease from ($|\psi_{max}| = 0.366$) to ($|\psi_{max}| = 0.125$). Therefore, it can be concluded that when the magnetic field acts in an inclined ($\gamma = 30^\circ$, 60°) and vertical ($\gamma = 90^\circ$) directions it causes to decelerate the flow circulation and the convection effect becomes weak. Furthermore, a clear disturbance can be observed in the flow vortices pattern when the magnetic field orientation angle increases. With respect to isotherms, a slight variation can be seen in the isotherms pattern when the magnetic field

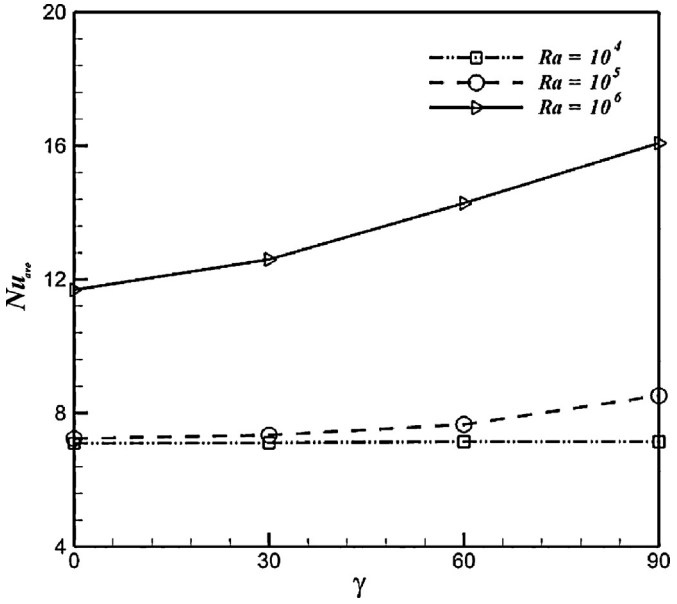

Fig. 11. Variation of average Nusselt number at different Rayleigh number and orientation angle (γ) at $\phi = 0.06$ and $Ha = 60$.

orientation angle increases. They are in general symmetrical and nearly parallel to the enclosure hot left sidewall indicating that conduction dominates the heat transfer process.

The variation of the average Nusselt number at different Rayleigh number and magnetic field orientation angle (γ) at $\varphi = 0.06$ (nanofluid) and $Ha = 60$ is illustrated in Fig. 11.It can be seen that the variation in the magnetic field orientation angle does not have any significant effect on the average Nusselt number values especially when the Rayleigh number is low. But, when the Rayleigh number is high, the average Nusselt number increases with the magnetic field orientation angle. From the other hand, the average Nusselt number increases when the Rayleigh number increases for all values of the magnetic field orientation angle. This is due to the convection effect which becomes very significant with increasing Rayleigh number and leads to increase the flow circulation strength and increases the temperature gradient adjacent the hot left sidewall and for this reason the average Nusselt number increases.

5. Conclusions

The following conclusions can be drawn from the results of the present work.

1. When the Rayleigh number is high and the Hartmann number is zero, the streamlines and isotherms are distributed strongly in the enclosure domain and the heat is transferred due to convection.
2. When the Rayleigh number is low and the Hartmann number is high, the isotherms are become smooth, symmetrical and parallel to the hot left sidewall indicating that the heat is transferred due to conduction.
3. The maximum stream function values and the flow circulation increase by adding the nano-particle to the fluid compared with their corresponding values of pure fluid.
4. The maximum stream function of the nanofluid begins to decrease as the Hartmann number increases for all values of the Rayleigh number.
5. The thermal boundary layer adjacent the hot left sidewall becomes thicker as the Rayleigh number increases.

6. When the magnetic field orientation angle increases, the flow circulation intensity and the convection effect begin to decrease. While, a slight variation can be seen in the isotherms pattern when the magnetic field orientation angle increases.
7. When the Rayleigh number is low; the magnetic field orientation angle does not have any significant influence on the average Nusselt number. But, when the Rayleigh number is high, the average Nusselt number increases with the magnetic field orientation angle.
8. The Nusselt number ratio increases when the Rayleigh number increases. From the other side, a different behavior can be seen for the Nusselt number ratio with the Hartmann number variation.

References

Abu-Nada, E., Masoud, Z., Hijazi, A., 2008. Natural convection heat transfer enhancement in horizontal concentric annuli using nanofluids. Int. Commun. Heat Mass Transfer 35, 657–665.

Aghajani Delavar, M., Farhadi, M., Sedighi, K., 2011. Effect of discrete heater at the vertical wall of the cavity over the heat transfer and entropy generation using lattice Boltzmann method. Therm. Sci. 15 (2), 423–435.

Bararnia, H., Hooman, K., Ganji, D.D., 2011. Natural convection in a nanofluids-filled portioned cavity: the lattice-Boltzmann method. Numer. Heat Transfer A 59, 487–502.

Chan, Y.L., Tien, C.L., 1985. A numerical study of two-dimensional laminar natural convection in shallow open cavities. Int. J. Heat Mass Transfer 28, 603–612.

Chang Feng, M.A., Bao Chang, S.H.I., Xing Wang, C.H., 2005. Lattice Bhatnagar gross Krook simulations in 2-D incompressible magnetohydrodynamics. Commun. Theor. Phys. 44, 917–920.

Dellar, P.J., 2002. Lattice kinetic schemes for magnetohydrodynamics. J. Comp. Phys. 179, 95–126.

Hasanpour, A., Farhadi, M., Sedighi, K., Ashorynejad, H.R., 2010. Lattice Boltzmann simulation for magneto hydrodynamic flow in a mixed convective flow in a porous medium. World Appl. Sci. J. 11 (9), 1124–1132.

Kakaç, S., Pramuanjaroenkij, A., 2009. Review of convective heat transfer-enhancement with nanofluids. Int. J. Heat Mass Transfer 52, 3187–3196.

Khanafer, K., Vafai, K., Lightstone, M., 2003. Buoyancy-driven heat transfer enhancement in a two-dimensional enclosure utilizing nanofluids. Int. J. Heat Mass Transfer 46, 3639–3653.

MacNab, A., Vahala, G., Pavlo, P., Vahala, L., Soe, M., 2001. Lattice Boltzmann model for dissipative incompressible MHD. In: 28th EPS Conference on Controlled Fusion and Plasma Physics, vol. 25A, Funchal, pp. 853–856.

Mahmoudi, A.H., Shahi, M., Shahedin, A.M., Hemati, N., 2011. Numerical modeling of natural convection in an open enclosure with two vertical thin heat sources subjected to a nanofluid. Int. Commun. Heat Mass Transfer 38, 110–118.

Mohamad, A.A., 1995. Natural convection in open cavities and slots. Numer. Heat Transfer 27, 705–716.

Mohamad, A.A., El-Ganaoui, M., Bennacer, R., 2009. Lattice Boltzmann simulation of natural convection in an open ended enclosure. Int. J. Therm. Sci. 48, 1870–1875.

Nemati, H., Farhadi, M., Sedighi, K., Fattahi, E., 2011. Multi-relaxation-time lattice Boltzmann model for uniform shear flow over a rotating circular cylinder. Therm. Sci. 15 (3), 859–878.

Ozoe, H., Okada, K., 1989. The effect of the direction of the external magnetic field on the three-dimensional natural convection in a cubical enclosures. Int. J. Heat Mass Transfer 32 (10), 1939–1954.

Oztop, H.F., Abu-Nada, E., 2008. Numerical study of natural convection in partially heated rectangular enclosures filled with nanofluids. Int. J. Heat Fluid Flow 29, 1326–1336.

Polat, O., Bilgen, E., 2002. Laminar natural convection in inclined open shallow cavities. Int. J. Therm. Sci. 41, 360–368.

Qi, J., Wakayama, N.I., Yabe, A., 1999. Attenuation of natural convection by magnetic force in electro-nonconducting fluids. J. Cryst. Growth 204, 408–412.

Rudraiah, N., Barron, R.M., Venkatachalappa, M., Subbaraya, C.K., 1995. Effect of a magnetic field on free convection in a rectangular enclosure. Int. J. Eng. Sci. 33 (8), 1075–1084.

Wang, X.Q., Mujumdar, A.S., 2007. Heat transfer characteristics of nanofluids: a review. Int. J. Therm. Sci. 46 (1), 1–19.

Xing-Wang, Ch., Bao Chang, Sh., 2005. A new lattice Boltzmann model for incompressible magneto hydrodynamics incompressible. Chin. Phys. 14 (7).

Xuan, Y., Roetzel, W., 2000. Conceptions for heat transfer correlation of nanofluids. Int. J. Heat Mass Transfer 43 (19), 3701–3707.